

Article

Not peer-reviewed version

---

# Eco-Friendly TiO<sub>2</sub> Nanoparticles: Harnessing Aloe Vera for Superior Photocatalytic Degradation of Methylene Blue

---

[Agnese De Luca](#) , Angeloantonio De Benedetto , [Mariafrancesca Cascione](#) <sup>\*</sup> , [Valeria De Matteis](#) <sup>\*</sup> ,  
[Riccardo Di Corato](#) , Massimo Corrado , [Rosaria Rinaldi](#)

Posted Date: 7 October 2024

doi: 10.20944/preprints202410.0488.v1

Keywords: green titanium dioxide nanoparticles; green synthesis; photocatalytic effects; Methylene Blue



Preprints.org is a free multidiscipline platform providing preprint service that is dedicated to making early versions of research outputs permanently available and citable. Preprints posted at Preprints.org appear in Web of Science, Crossref, Google Scholar, Scilit, Europe PMC.

Copyright: This is an open access article distributed under the Creative Commons Attribution License which permits unrestricted use, distribution, and reproduction in any medium, provided the original work is properly cited.

Article

# Eco-Friendly TiO<sub>2</sub> Nanoparticles: Harnessing *Aloe Vera* for Superior Photocatalytic Degradation of Methylene Blue

Agnese De Luca<sup>1</sup>, Angelantonio De Benedetto<sup>1</sup>, Mariafrancesca Cascione<sup>1,2,\*</sup>,  
Valeria De Matteis<sup>1,2,\*</sup>, Riccardo Di Corato<sup>2,3</sup>, Massimo Corrado<sup>1</sup> and Rosaria Rinaldi<sup>1,2</sup>

<sup>1</sup> Department of Mathematics and Physics "Ennio De Giorgi", University of Salento, Via Arnesano, 73100 Lecce (LE), Italy

<sup>2</sup> Institute for Microelectronics and Microsystems (IMM), CNR, Via Monteroni, Lecce, 73100, Italy

<sup>3</sup> Center for Biomolecular Nanotechnologies, Istituto Italiano di Tecnologia, Arnesano 73010, Italy

\* Corresponding authors: valeria.dematteis@unisalento.it; mariafrancesca.cascione@unisalento.it

† These authors equally contributed to the work.

**Abstract:** In recent years; the contamination of aquatic environments by organic chemicals has become an increasing concern. To effectively remove toxic pollutants and biologically resistant compounds; a combination of advanced technologies must complement conventional methods. Indeed; among environmental pollutants; dyes such as methylene blue (MB); congo red and crystal violet persist in the environment because they are difficult to biodegrade. Advanced oxidation processes (AOPs) are widely employed to treat various types of wastewaters; often in conjunction with biological treatments. Among these technologies; heterogeneous photocatalysis stands out as one of the most extensively studied; with Titanium dioxide being the most researched photocatalyst due to its high photoactivity. In this study; Titanium dioxide nanoparticles (NPs) were synthesized using both a green method; leveraging the natural properties of Aloe vera leaf extract; and a conventional approach. The resulting NPs were thoroughly characterized using XRD; TEM; and  $\zeta$ -potential analysis. Their photocatalytic performance was assessed by measuring the degradation of MB under UV light. The TiO<sub>2</sub> NPs synthesized via the green method demonstrated a degradation efficiency of  $(50 \pm 3)$  % after 180 minutes; significantly higher than the  $(16 \pm 3)$ % achieved by NPs synthesized through the conventional route. Moreover; the reaction rate constant for the green-synthesized TiO<sub>2</sub> NPs was found to be approximately five times greater than that of the conventionally synthesized NPs. These results open new scenario in the pollution removing strategy research

**Keywords:** green titanium dioxide nanoparticles; green synthesis; photocatalytic effects; Methylene Blue

## 1. Introduction

In recent years, the aquatic environment has been found to be contaminated by organic chemicals such as industrial chemicals, pharmaceuticals and consumer products [1]. These substances are only partially removed through conventional physical and biological wastewater treatment, necessitating the use of additional technologies are necessary to eliminate toxic pollutants and biologically recalcitrant compounds [2]. For instance, synthetic dyes, such as congo red, toluidine blue, crystal violet and methylene blue, are difficult to biodegrade, so they remain in the environment [3]. Advanced oxidation processes (AOPs) are widely employed for treating various types of wastewaters, often in conjunction with biological treatments [4]. AOPs facilitate the in-situ generation of strong oxidants that enable the oxidation of organic compounds [5]. Different AOPs utilize different mechanisms for organic destruction and can be classified into ozone-based, UV-based,

catalytic (cAOP), physical (pAOP) and electrochemical (eAOP) AOPs [6]. Heterogeneous photocatalysis is the one of the most investigated AOP [7,8]. It involves the creation of electron-hole pairs through the absorption of photons with energy equal to or greater than the semiconductor bandgap [9]. If electron-hole recombination does not occur, these charge carriers can induce redox reaction with adsorbed species on the semiconductor surface, producing radical species such as hydroxyl radical, superoxide radical anions, and other reactive oxygen species that facilitate the degradation of pollutants [10]. Among several semiconductors, titanium dioxide ( $\text{TiO}_2$ ) is the most thoroughly investigated due to its properties, such as its chemical and thermal stability, high photoactivity, cost-effectiveness, and low toxicity [11].  $\text{TiO}_2$  occurs in nature in four polymorphisms: anatase, rutile, both with a tetragonal crystal structure, brookite, with an orthorhombic geometry, and  $\text{TiO}_2(\text{B})$ , the monoclinic phase of titanium dioxide [12]. Anatase and rutile are the most commonly occurred forms [13], finding numerous applications including photocatalysis. The photocatalytic activity of  $\text{TiO}_2$  depends on several factors, including phase structure, crystallite size, specific surface area and pore structure [14]. Anatase exhibits considerably higher photocatalytic activity than rutile [15]. Several strategies can be employed to obtain nanoparticles (NPs) of  $\text{TiO}_2$  [16], including sol-gel, hydrothermal, and solvothermal methods. For instance, Collazzo et al. used the hydrothermal method with titanium tetraisopropoxide (TTIP) as precursor in order to obtain  $\text{TiO}_2$  nanopowders with a crystallite size ranging from 9 to 17 nm, depending on the synthesis conditions such as temperature and reaction time [17]. Li et al. prepared nano- $\text{TiO}_2$  powders by sol-gel method using tetra-n-butyl-titanate as precursor, investigating different synthesis parameters such as calcination temperature and pH value, to control the grain size and microstructure of nano- $\text{TiO}_2$  powders [18]. Xu et al. synthesized nano- $\text{TiO}_2$  from Tetrabutyl titanate (n-TBT) [19], obtaining NPs with a homogeneous microstructure and a size of around 10–15 nm through a sol-gel process mediated in reverse microemulsion combined with a solvent thermal technique. Sadek et al. used TTIP to prepare  $\text{TiO}_2$  nanopowders with a crystal size of 49.3 nm through the sol-gel method [20]. Currently, the growing use of NPs in various applications has stimulated the development of more inexpensive and sustainable synthesis approach. In particular, green approach [21], based on the use of natural source materials, allows for the elimination or reduction of chemical reagents and the generation of hazardous substances [22]. The green synthesis can be carried out by means of the use of plants and their extracts as well as the microbes, although the former is considered more stable [23]. Several part of the plant, such as flowers, roots, seeds, and leaves can be employed to prepare plant extracts, though leaves are more commonly used. Leaves are rich in biomolecules such as proteins, amino acids, terpenoids, flavonoids, saponins. These molecules are key elements in the synthesis of nanoparticles because they act as a reducing agents and capping agents, as stabilizer and redox mediators. Santhoshkumar et al. prepared  $\text{TiO}_2$  NPs using  $\text{TiO}(\text{OH})_2$  as precursor and the aqueous extract of *Psidium guajava* leaves [24]. Ahmad et al. synthesized spherical  $\text{TiO}_2$  NPs ranging from 20 to 70 nm using TTIP and *Mentha arvensis* leaves extract as precursor and reducing agent, respectively [25]. Saini et Kumar achieved the green synthesis of  $\text{TiO}_2$  NPs, with an average crystallite size of 15.02 nm, by mixing the *Tinospora cordifolia* leaves extract to the precursor, TTIP [26]. Rao et al. prepared  $\text{TiO}_2$  NPs with an estimated average particle size of 32 nm by using Titanium Chloride ( $\text{TiCl}_4$ ) and *Aloe Vera* leaf extract [27]. In this context  $\text{TiO}_2$  NPs have been synthesized via both a green route using *Aloe Vera* leaves extract and a conventional route. The properties of the obtained NPs were characterized by different techniques, specifically Transmission Electron Microscopy (TEM), X-Ray Diffraction (XRD), Fourier Transform Infrared Spectroscopy (FTIR) and  $\zeta$ -potential measurements. Moreover, the photocatalytic activity of NPs was evaluated by the degradation of methylene blue (MB) under UV light. MB was chosen because it is a popular cationic dye frequently used for dyeing (clothes, paper and leathers) and in the textile industry [3] and it is harmful to human health above a certain concentration [28]. Additionally, the effect of the calcination temperature for  $\text{TiO}_2$  NPs synthesized by the green route was investigated.

## 2. Materials and Methods

### 2.1. Reagents

Titanium (IV) isopropoxide (TTIP, 97%), ethanol absolute ( $\geq 99.8\%$ ), 2-propanol ( $\geq 99.8\%$ ), nitric acid ( $\text{HNO}_3$  65%), ultrapure water (produced by Barnstead Smart2Pure water purification system Thermo Scientific), methylene blue hydrate.

## 2.2. Synthesis of $\text{TiO}_2$ NPs

### 2.2.1. Conventional route for Synthesis of $\text{TiO}_2$ NPs ( $\text{TiO}_2$ -Chem NPs)

$\text{TiO}_2$  NPs was synthesized following the method described in [29] by sol-gel route. 1 mL of TTIP was slowly added to 5 mL of 25% (v/v) ethanol aqueous solution. The mixture was kept under stirring for 60 min, then the pH was adjusted to 2-3 by adding nitric acid and it was kept under stirring for 60 min. Afterwards, the mixture was dried in an oven using two steps: 120 °C for 120 min and then at 270 °C for 24 h. Finally, the obtained  $\text{TiO}_2$  NPs were ground with a mortar. In Figure 1 (on the left) the flow chart of the synthesis process is shown.

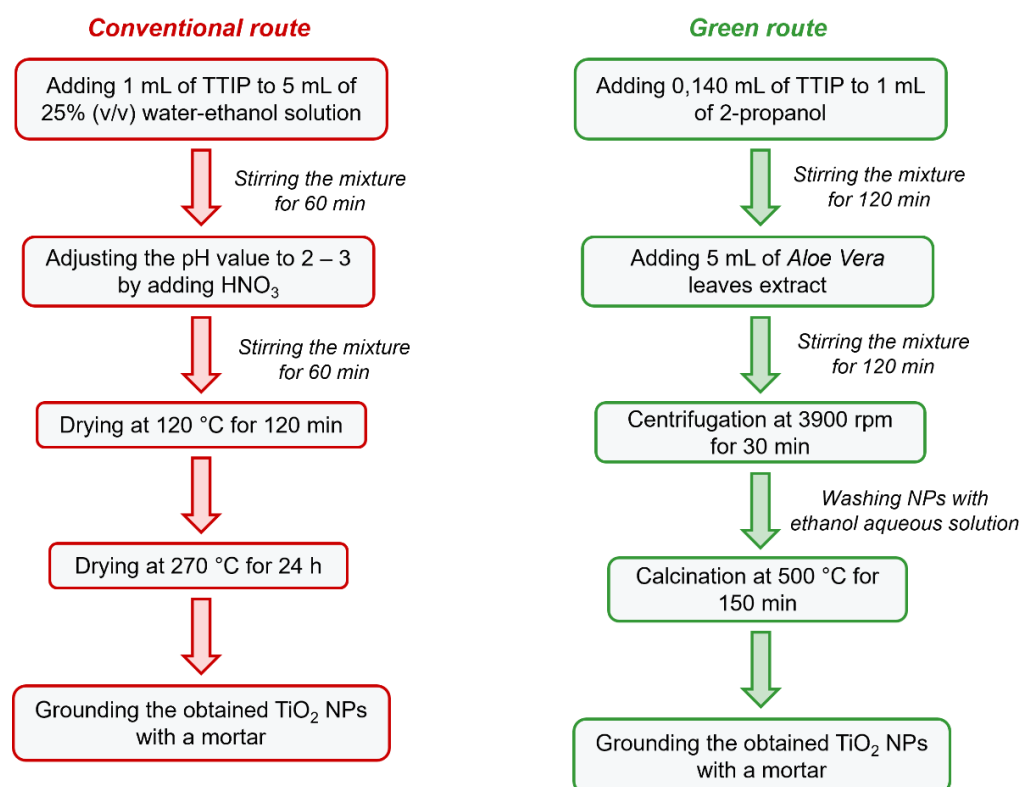


**Figure 1.** Flow charts concerning the synthesis of  $\text{TiO}_2$  NPs: conventional route (on the left) and green route (on the right).

### 2.2.2. Green Synthesis of $\text{TiO}_2$ NPs ( $\text{TiO}_2$ -Green NPs)

#### Preparation of the Leaves Extract

*Aloe vera* leaves was separated from the gel and washed with ultrapure water. After drying at room temperature, they were cut into small pieces. Then, 25 g of leaves were transferred into a glass flask containing 250 mL of ultrapure water and the mixture was boiled at 100 °C for 20 min. After cooling, the mixture was filtered by Whatman filter.

#### Synthetic Procedure

0.140 mL of TTIP was slowly added to 1 mL of 2-propanol and the solution was kept under stirring for 120 min. Then, 5 mL of the *Aloe vera* leaves extract were slowly added to the solution and the obtained mixture was kept under stirring for 120 min. Afterwards,  $\text{TiO}_2$  NPs were collected by centrifugation at 3900 rpm for 30 min. The collected NPs were washed 4-5 times with 50% (v/v) ethanol aqueous solution, then the  $\text{TiO}_2$  NPs were calcined at 500 °C for 150 min. Lastly, the  $\text{TiO}_2$  NPs were ground with a mortar. The flow chart the synthesis process is shown in Figure 1 (on the right).

### 2.3. Characterization of TiO<sub>2</sub> NPs

#### 2.3.1. Transmission Electron Microscopy (TEM) Analysis

TEM characterizations were performed by a JEOL JEM-1011 transmission electron microscope operating at 100 kV. For both synthesized TiO<sub>2</sub> NPs, samples were prepared by dropping a dilute suspension of TiO<sub>2</sub> NPs in ultrapure water on TEM grid and drying overnight at room temperature.

#### 2.3.2. Zeta Potential Analysis

ζ-potential analysis was performed at 25 °C by Zetasizer Nano-ZS (Model ZEN3600, Malver Instruments Ltd., Malvern, UK) equipped with a HeNe laser working at 663 nm. Each suspension of TiO<sub>2</sub> NPs (0.4 mg/mL) in ultrapure water was prepared for the measurements.

#### 2.3.3. X-Ray Diffraction (XRD) Analysis

X-ray diffraction analysis was performed in Bragg-Brentano reflection geometry using filtered Cu-Kα radiation. The X-ray diffraction data were collected at a scanning rate of 0.02 degrees per second in 2θ ranging from 20° to 80° by step scanning.

### 2.4. Assessment of Photocatalytic Activity

The photocatalytic activity of the synthesized TiO<sub>2</sub> NPs was evaluated by the degradation of MB in aqueous solution. With this aim, an UV irradiator (Figure 2), equipped with 2 UV lamps (8W, λ=365 nm) and a magnetic stirrer, was used. A suspension of the TiO<sub>2</sub> NPs with a concentration of 0.4 g/L was prepared in 5 mg/L methylene blue solution and it was homogenized by sonication for 60 s. The suspension was kept under stirring and under dark condition for 30 min to achieve the adsorption-desorption equilibrium, then it was exposed to UV light under stirring condition at a distance from the UV source of about 12.5 cm and samples were taken at different times: 0 min, 30 min, 60 min, 90 min, 120 min, 180 min. Afterwards, the collected samples were centrifuged in order to remove the nanoparticles and the absorption spectra of the samples were acquired by BioTek Synergy Mx multi-mode microplate reader. The absorption maximum at 664 nm was used in order to monitor the dye degradation over time.



**Figure 2.** Pictures of the UV irradiator used for the photocatalysis experiments.

## 3. Results and Discussion

The findings of this study underscore the potential of green synthesis methods for TiO<sub>2</sub> NPs production in enhancing the efficiency of photocatalytic processes for environmental remediation. In particular we have focused on Methylene blue that is considered a potent pollutant due to several factors. Indeed, it is highly toxic to aquatic life, even at low concentrations, disrupting ecosystems by

affecting the health and reproduction of various species [30]. Additionally, methylene blue is resistant to biodegradation, meaning it can persist in the environment for extended periods, leading to long-term contamination of water bodies [31]. It also absorbs strongly in the visible spectrum, which can block sunlight from penetrating the water, inhibiting photosynthesis in aquatic plants and algae, further disturbing the balance of aquatic ecosystems [3,32]. Moreover, methylene blue can enter the human food chain through contaminated water sources, posing health risks to humans and animals [33,34]. These characteristics make it a significant concern for environmental pollution. Titanium dioxide (TiO<sub>2</sub>) nanoparticles are crucial in the photocatalysis of methylene blue due to their unique properties and effectiveness in breaking down organic pollutants [35,36]. TiO<sub>2</sub> exhibits exceptional photocatalytic activity when exposed to UV light. Its wide bandgap allows it to generate electron-hole pairs upon irradiation, which are essential for initiating the oxidation and reduction reactions necessary to degrade organic compounds like methylene blue [37,38]. Therefore, the synthetic processes required the use for toxic substances and time-consuming equipment's. Then, the development of environmentally friendly method to obtain TiO<sub>2</sub> NPs highly efficient is necessary in order to making it a safe option for treating wastewater without introducing additional harmful substances into the environment [21,39]. In our work we obtained TiO<sub>2</sub> NPs from a conventional route and green route using, in the last case *Aloe Vera* leaf extract. This plant is widely distributed in the Mediterranean region and is extensively used in the agricultural, biomedical, and cosmetic fields. In the latter case, in particular, the gel found in the leaves is a valuable material often used to produce skin and beauty lotions. On the other hand, the leaf epidermis, which is considered a waste product, contains high concentrations of vitamins, proteins, and polyphenols, and its extract can be used to produce TiO<sub>2</sub> NPs. The fito molecules enriched the extracts acting as reducing and capping agent [40,41]. Then, we proceed to achieve TiO<sub>2</sub> NPs from the two different routes described in the Materials section following the characterization of their physico-chemical properties. Firstly, we investigated about TEM analysis (Figure 3) showed that synthesized TiO<sub>2</sub> NPs showed an irregular shape as also reported in literature [42–44]. It was observed that the synthesized NPs had similar size. An average size of (12 ± 3) nm for the TiO<sub>2</sub>-chem NPs and an average size of (12 ± 4) nm for the TiO<sub>2</sub>-green NPs were estimated. However, aggregation phenomena were also observed, which were more evident in the case of TiO<sub>2</sub>-green NPs probably due to the high concentration of organic compounds enriched the leaves extract.

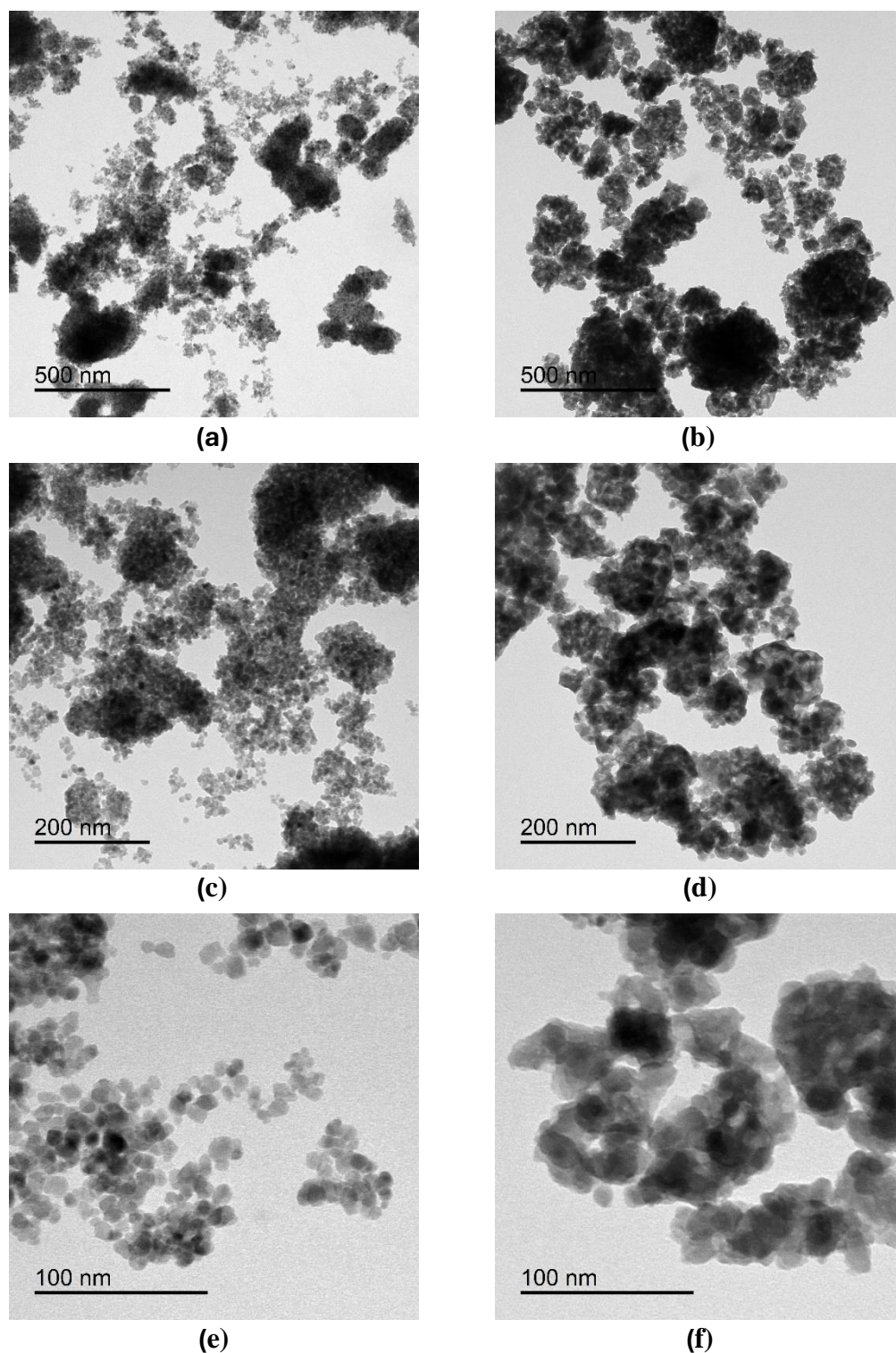


**Figure 3.** Representative TEM images of TiO<sub>2</sub>-chem NPs on the left (a, c, e), TiO<sub>2</sub>-green NPs on the right (b, d, f).

Both synthesized TiO<sub>2</sub> NPs showed a negative surface charge in ultrapure water at neutral pH. Z-potential values of  $(-18.2 \pm 0.2)$  mV and  $(-28.4 \pm 0.9)$  mV were observed for TiO<sub>2</sub>-chem and TiO<sub>2</sub>-green NPs, respectively. Therefore, adsorption of MB is expected to be favoured on the surface of the synthesized NPs, since MB is a cationic dye [45,46].

The XRD pattern of the synthesized TiO<sub>2</sub> NPs (Figure 4) showed characteristic peaks of anatase for both TiO<sub>2</sub>-chem and TiO<sub>2</sub>-green NPs around the following 2θ values: 25.4° (101), 37.9° (004), 48.1°(200), 62.9°(204). Two small characteristic peaks of rutile phase, around 27.5° (110) and 36.2° (110) were observed only for the TiO<sub>2</sub>-green NPs [47,48]. In addition, a small peak around 30.8° (121), that can be related to brookite phase [49], was also observed for both TiO<sub>2</sub> NPs. The anatase phase generally has higher photocatalytic performance than that of rutile due to a higher density of localized states and consequent surface-adsorbed hydroxyl radicals and lower recombination of photogenerated electrons and holes in anatase than in rutile [50].

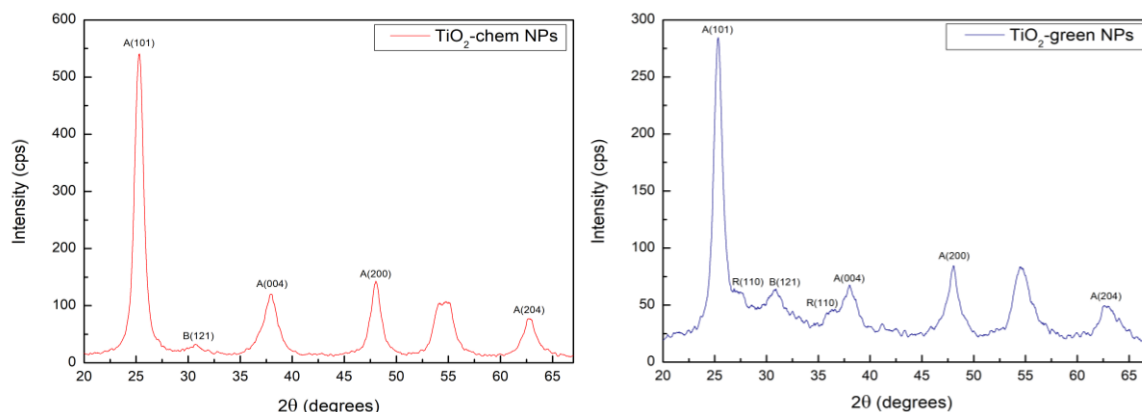


**Figure 4.** XRD pattern of TiO<sub>2</sub>-chem NPs (on the left) and TiO<sub>2</sub>-green NPs (on the right).

After the TiO<sub>2</sub> characterization, we perform the assessment of their photocatalytic activity. The photocatalytic activity of the synthesized TiO<sub>2</sub> NPs was evaluated by the degradation of MB in aqueous solution under UV light (Figure 5, upper image). As shown in lower image of Figure 5, it was found that the kinetics of the photocatalytic degradation follow a pseudo-first-order model (equation 1):

$$\ln\left(\frac{C_t}{C_0}\right) = -k \cdot t$$

where  $C_t$  is the concentration of MB at time  $t$ ,  $C_0$  is the concentration of MB at time  $t = 0$  and  $k$  is the reaction rate constant. The reaction rate constant for TiO<sub>2</sub>-green NPs was about 5 times higher than that for TiO<sub>2</sub>-chem NPs. As shown in Table 1, the reaction rate constants were 0.004 min<sup>-1</sup> and 0.0008 min<sup>-1</sup> for TiO<sub>2</sub>-green and TiO<sub>2</sub>-chem NPs, respectively. The degradation efficiency was calculated using the following equation 2:

$$\text{Degradation efficiency}(\%) = \left(\frac{C_0 - C_t}{C_0}\right) \cdot 100$$

where  $C_0$  is the concentration of MB at time  $t = 0$  and  $C_t$  is the concentration of MB at time  $t$ .

As shown in Table 1, the TiO<sub>2</sub>-green NPs showed higher efficiency for MB degradation than the TiO<sub>2</sub>-chem NPs. In fact, the degradation efficiency values obtained after 180 min were (50 ± 3) % and (16 ± 3) % for TiO<sub>2</sub>-green and TiO<sub>2</sub>-chem NPs, respectively.

The higher negative ζ-potential value of TiO<sub>2</sub>-green NPs, compared with TiO<sub>2</sub>-chem NPs, may suggest an improvement in the adsorption of cationic organic pollutants leading to an enhancement of photocatalytic efficiency [51]. Moreover, the small rutile content found for TiO<sub>2</sub>-green NPs may indicate that the enhancement of the photocatalytic activity may also be due to charge transfer effects in mixed phase TiO<sub>2</sub> (anatase/rutile) that improve the charge separation of photogenerated carriers [52,53].

**Table 1.** Degradation values after 180 min and reaction rate constants for TiO<sub>2</sub> NPs synthesized by green route (TiO<sub>2</sub>-green NPs) and by conventional route (TiO<sub>2</sub>-chem NPs).

Catalyst	Degradation after 180 min	K
TiO <sub>2</sub> -green NPs	(50 ± 3) %	0.004 min <sup>-1</sup>
TiO <sub>2</sub> -chem NPs	(16 ± 3) %	0.0008 min <sup>-1</sup>

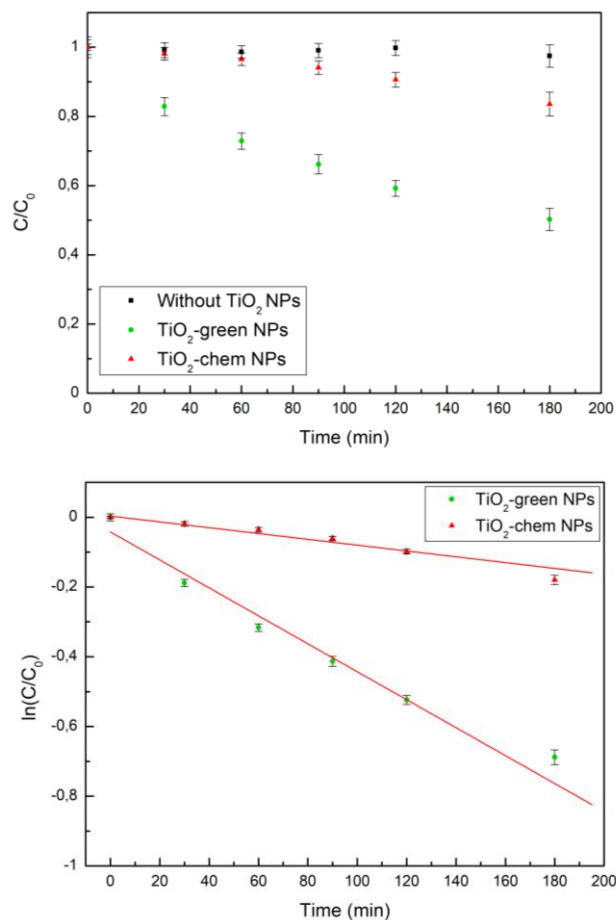


**Figure 5.** Photocatalytic degradation of MB as a function of time under UV light (upper image) and pseudo first-order kinetics (lower image). The slope of the fitted lines gave the values of the reaction rate constants:  $0.004 \text{ min}^{-1}$  ( $R^2= 0.97$ ) for TiO<sub>2</sub>-green NPs (green circles) and  $0.0008 \text{ min}^{-1}$  ( $R^2= 0.95$ ) for TiO<sub>2</sub>-chem NPs (red triangles).

The effect of calcination temperature on TiO<sub>2</sub>-green NPs was also analyzed by the evaluation of the photocatalytic activity of the synthesized NPs. As shown in Figure 6, it was observed that the TiO<sub>2</sub>-green NPs calcined at 500 °C showed higher degradation efficiency than the TiO<sub>2</sub> NPs calcined at 400 °C. This can be due to the residual organic material on the surface of NPs calcined at 400 °C. The degradation efficiency values obtained after 180 min were  $(50 \pm 3) \%$  for the TiO<sub>2</sub> NPs calcined at 500 °C and  $(10 \pm 4) \%$  for the TiO<sub>2</sub> NPs calcined at 400 °C. A fine white powder was obtained by calcination process at 500 °C, whereas a gray powder with large grains was observed for TiO<sub>2</sub> NPs calcined at 400 °C, maybe due to residual carbon from organic compounds of the leaves extract. The excess of residual carbon material on the surface of NPs calcined at 400 °C can cover part of the photocatalyst, leading to an impediment of light access and reactants access to the photocatalyst surface [54], resulting in a decreased photocatalytic efficiency.

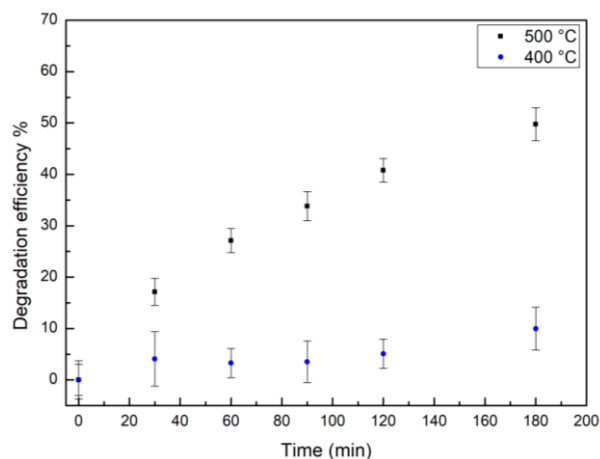


**Figure 6.** Photocatalytic degradation of MB under UV light: degradation efficiency as a function of time using TiO<sub>2</sub>-green NPs calcined at 500 °C (black squares) and calcined at 400 °C (blue circles).

#### 4. Conclusions

In this work, TiO<sub>2</sub> NPs were synthesized, and their photocatalytic activity was evaluated by the degradation of MB in aqueous solution, under UV light. TiO<sub>2</sub> NPs were synthesized by means of two approaches using TTIP as precursor: a green route exploiting the properties of *Aloe vera* leaves extract and a conventional synthesis. Both types of TiO<sub>2</sub> NPs showed irregular shape and aggregation phenomena. The TiO<sub>2</sub>-green NPs showed characteristic peaks of anatase phase, two small characteristic peaks of rutile phase and a small peak that can be related to brookite phase, whereas TiO<sub>2</sub>-chem NPs showed only characteristic peaks of anatase phase and a small peak that can be related to brookite phase.  $\zeta$ -potential analysis showed that both synthesized TiO<sub>2</sub> NPs had a negative surface charge with a higher negative value of TiO<sub>2</sub>-green NPs compared with TiO<sub>2</sub>-chem NPs. Concerning the evaluation of the photocatalytic activity by the degradation of MB in aqueous solution, the reaction rate constant for TiO<sub>2</sub>-green NPs was about 5 times higher than that for TiO<sub>2</sub>-chem NPs. In fact, the degradation efficiency values obtained after 180 min were (50 ± 3)% for TiO<sub>2</sub>-green NPs and (16 ± 3)% for TiO<sub>2</sub>-chem NPs. The high photocatalytic activity exhibited by TiO<sub>2</sub>-green NPs compared with TiO<sub>2</sub>-chem NPs may be due to a higher negative surface charge. This can improve the adsorption of cationic organic pollutants and may be due to charge transfer effects in mixed phase TiO<sub>2</sub> (anatase/rutile) that enhance the charge separation of photogenerated carries.

**Data Availability Statement:** The data presented in this study are available in this article.

**Conflicts of Interest:** There are no conflicts to declare.

**Author Contributions:** V.D.M and Mf.C Conceptualization, Methodology, Supervision, data analysis, editing draft of manuscript; A.D.L synthesized the nanomaterials, A.D.B and A.D.L. methodology, writing original manuscript; R.D.C. methodology and data analysis; M.C methodology; RR funding and supervision.

**Funding:** VDM kindly acknowledges Programma Operativo Nazionale (PON) Ricerca e Innovazione 2014–2020 Azione IV.6 “Contratti su tematiche green”-DM 1062/2021 for sponsoring her salary and work.

#### References

1. M. Huerta-Fontela, M. T. Galceran, e F. Ventura, «Fast liquid chromatography–quadrupole-linear ion trap mass spectrometry for the analysis of pharmaceuticals and hormones in water resources», *J. Chromatogr. A*, vol. 1217, fasc. 25, pp. 4212–4222, giu. 2010, doi: 10.1016/j.chroma.2009.11.007.
2. R. Andreatti, «Advanced oxidation processes (AOP) for water purification and recovery», *Catal. Today*, vol. 53, fasc. 1, pp. 51–59, ott. 1999, doi: 10.1016/S0920-5861(99)00102-9.
3. P. O. Oladoye, T. O. Ajiboye, E. O. Omotola, e O. J. Oyewola, «Methylene blue dye: Toxicity and potential elimination technology from wastewater», *Results Eng.*, vol. 16, p. 100678, dic. 2022, doi: 10.1016/j.rineng.2022.100678.

4. Y. Deng e R. Zhao, «Advanced Oxidation Processes (AOPs) in Wastewater Treatment», *Curr. Pollut. Rep.*, vol. 1, fasc. 3, pp. 167–176, set. 2015, doi: 10.1007/s40726-015-0015-z.
5. J. R. Bolton, K. G. Bircher, W. Tumas, e C. A. Tolman, «Figures-of-merit for the technical development and application of advanced oxidation technologies for both electric- and solar-driven systems (IUPAC Technical Report)», *Pure Appl. Chem.*, vol. 73, fasc. 4, pp. 627–637, gen. 2001, doi: 10.1351/pac200173040627.
6. D. B. Miklos, C. Remy, M. Jekel, K. G. Linden, J. E. Drewes, e U. Hübner, «Evaluation of advanced oxidation processes for water and wastewater treatment – A critical review», *Water Res.*, vol. 139, pp. 118–131, ago. 2018, doi: 10.1016/j.watres.2018.03.042.
7. Y. Zhang, B. Zhou, H. Chen, e R. Yuan, «Heterogeneous photocatalytic oxidation for the removal of organophosphorus pollutants from aqueous solutions: A review», *Sci. Total Environ.*, vol. 856, p. 159048, gen. 2023, doi: 10.1016/j.scitotenv.2022.159048.
8. H. Wang *et al.*, «A review on heterogeneous photocatalysis for environmental remediation: From semiconductors to modification strategies», *Chin. J. Catal.*, vol. 43, fasc. 2, pp. 178–214, feb. 2022, doi: 10.1016/S1872-2067(21)63910-4.
9. S. San Martín, M. J. Rivero, e I. Ortiz, «Unravelling the Mechanisms that Drive the Performance of Photocatalytic Hydrogen Production», *Catalysts*, vol. 10, fasc. 8, p. 901, ago. 2020, doi: 10.3390/catal10080901.
10. M. Pelaez *et al.*, «A review on the visible light active titanium dioxide photocatalysts for environmental applications», *Appl. Catal. B Environ.*, vol. 125, pp. 331–349, ago. 2012, doi: 10.1016/j.apcatb.2012.05.036.
11. M. V. Shinnur, M. Pedferri, e M. V. Diamanti, «Properties and photocatalytic applications of black TiO<sub>2</sub> produced by thermal or plasma hydrogenation», *Curr. Res. Green Sustain. Chem.*, vol. 8, p. 100415, 2024, doi: 10.1016/j.crgsc.2024.100415.
12. Y. Ma, X. Wang, Y. Jia, X. Chen, H. Han, e C. Li, «Titanium Dioxide-Based Nanomaterials for Photocatalytic Fuel Generations», *Chem. Rev.*, vol. 114, fasc. 19, pp. 9987–10043, ott. 2014, doi: 10.1021/cr500008u.
13. D. R. Eddy *et al.*, «Heterophase Polymorph of TiO<sub>2</sub> (Anatase, Rutile, Brookite, TiO<sub>2</sub> (B)) for Efficient Photocatalyst: Fabrication and Activity», *Nanomaterials*, vol. 13, fasc. 4, p. 704, feb. 2023, doi: 10.3390/nano13040704.
14. J. Yu *et al.*, «Effects of acidic and basic hydrolysis catalysts on the photocatalytic activity and microstructures of bimodal mesoporous titania», *J. Catal.*, vol. 217, fasc. 1, pp. 69–78, lug. 2003, doi: 10.1016/S0021-9517(03)00034-4.
15. A. L. Linsebigler, G. Lu, e J. T. Yates, «Photocatalysis on TiO<sub>2</sub> Surfaces: Principles, Mechanisms, and Selected Results», *Chem. Rev.*, vol. 95, fasc. 3, pp. 735–758, mag. 1995, doi: 10.1021/cr00035a013.
16. I. F. Mironyuk, L. M. Soltys, T. R. Tatarchuk, e Kh. O. Savka, «Methods of Titanium Dioxide Synthesis (Review)», *Phys. Chem. Solid State*, vol. 21, fasc. 3, pp. 462–477, set. 2020, doi: 10.15330/pcss.21.3.462-477.
17. G. C. Collazzo, S. L. Jahn, N. L. V. Carreño, e E. L. Foletto, «Temperature and reaction time effects on the structural properties of titanium dioxide nanopowders obtained via the hydrothermal method», *Braz. J. Chem. Eng.*, vol. 28, fasc. 2, pp. 265–272, giu. 2011, doi: 10.1590/S0104-66322011000200011.
18. B. Li, X. Wang, M. Yan, e L. Li, «Preparation and characterization of nano-TiO<sub>2</sub> powder», *Mater. Chem. Phys.*, 2002.
19. H. Xu, M. Li, e Z. Jun, «Preparation, characterization, and photocatalytic studies on anatase nano-TiO<sub>2</sub> at internal air lift circulating photocatalytic reactor», *Mater. Res. Bull.*, vol. 48, fasc. 9, pp. 3144–3148, set. 2013, doi: 10.1016/j.materresbull.2013.04.075.
20. O. Sadek *et al.*, «Synthesis by sol-gel method and characterization of nano-TiO<sub>2</sub> powders», *Mater. Today Proc.*, vol. 66, pp. 456–458, 2022, doi: 10.1016/j.matpr.2022.06.385.
21. V. Verma, M. Al-Dossari, J. Singh, M. Rawat, M. G. M. Kordy, e M. Shaban, «A Review on Green Synthesis of TiO<sub>2</sub> NPs: Photocatalysis and Antimicrobial Applications», *Polymers*, vol. 14, fasc. 7, p. 1444, apr. 2022, doi: 10.3390/polym14071444.
22. P. T. Anastas, «Green Chemistry and the Role of Analytical Methodology Development», *Crit. Rev. Anal. Chem.*, vol. 29, fasc. 3, pp. 167–175, set. 1999, doi: 10.1080/10408349891199356.
23. P. Singh, Y.-J. Kim, D. Zhang, e D.-C. Yang, «Biological Synthesis of Nanoparticles from Plants and Microorganisms», *Trends Biotechnol.*, vol. 34, fasc. 7, pp. 588–599, lug. 2016, doi: 10.1016/j.tibtech.2016.02.006.
24. T. Santhoshkumar *et al.*, «Green synthesis of titanium dioxide nanoparticles using Psidium guajava extract and its antibacterial and antioxidant properties», *Asian Pac. J. Trop. Med.*, vol. 7, fasc. 12, pp. 968–976, dic. 2014, doi: 10.1016/S1995-7645(14)60171-1.
25. W. Ahmad, K. K. Jaiswal, e S. Soni, «Green synthesis of titanium dioxide (TiO<sub>2</sub>) nanoparticles by using *Mentha arvensis* leaves extract and its antimicrobial properties», *Inorg. Nano-Met. Chem.*, vol. 50, fasc. 10, pp. 1032–1038, ott. 2020, doi: 10.1080/24701556.2020.1732419.
26. R. Saini e P. Kumar, «Green synthesis of TiO<sub>2</sub> nanoparticles using *Tinospora cordifolia* plant extract & its potential application for photocatalysis and antibacterial activity», *Inorg. Chem. Commun.*, vol. 156, p. 111221, ott. 2023, doi: 10.1016/j.inoche.2023.111221.

27. K. G. Rao, C. Ashok, K. V. Rao, e C. S. Chakra, «Green Synthesis of TiO<sub>2</sub> Nanoparticles Using Aloe Vera Extract».
28. J. Cheng *et al.*, «Highly Efficient Removal of Methylene Blue Dye from an Aqueous Solution Using Cellulose Acetate Nanofibrous Membranes Modified by Polydopamine», *ACS Omega*, vol. 5, fasc. 10, pp. 5389–5400, mar. 2020, doi: 10.1021/acsomega.9b04425.
29. M. Leena e S. Srinivasan, «Synthesis and ultrasonic investigations of titanium oxide nanofluids», *J. Mol. Liq.*, vol. 206, pp. 103–109, giu. 2015, doi: 10.1016/j.molliq.2015.02.001.
30. S. Li, Y. Cui, M. Wen, e G. Ji, «Toxic Effects of Methylene Blue on the Growth, Reproduction and Physiology of *Daphnia magna*», *Toxics*, vol. 11, fasc. 7, p. 594, lug. 2023, doi: 10.3390/toxics11070594.
31. S. Modi *et al.*, «Recent and Emerging Trends in Remediation of Methylene Blue Dye from Wastewater by Using Zinc Oxide Nanoparticles», *Water*, vol. 14, fasc. 11, p. 1749, mag. 2022, doi: 10.3390/w14111749.
32. A. Krishna Moorthy, B. Govindarajan Rath, S. P. Shukla, K. Kumar, e V. Shree Bharti, «Acute toxicity of textile dye Methylene blue on growth and metabolism of selected freshwater microalgae», *Environ. Toxicol. Pharmacol.*, vol. 82, p. 103552, feb. 2021, doi: 10.1016/j.etap.2020.103552.
33. I. Khan *et al.*, «Review on Methylene Blue: Its Properties, Uses, Toxicity and Photodegradation», *Water*, vol. 14, fasc. 2, p. 242, gen. 2022, doi: 10.3390/w14020242.
34. N. Yahaya, I. Ali, K. Modu, e S. Adamu, «Adsorption Study of Methylene Blue onto Power Activated Carbon Prepared from Ananas Comosus Peels», *Nanochemistry Res.*, vol. 8, fasc. 4, ott. 2023, doi: 10.22036/NCR.2023.04.01.
35. S. A. Yasin, J. A. Abbas, M. M. Ali, I. A. Saeed, e I. H. Ahmed, «Methylene blue photocatalytic degradation by TiO<sub>2</sub> nanoparticles supported on PET nanofibres», *Mater. Today Proc.*, vol. 20, pp. 482–487, 2020, doi: 10.1016/j.matpr.2019.09.174.
36. L. Niu *et al.*, «Difference in performance and mechanism for methylene blue when TiO<sub>2</sub> nanoparticles are converted to nanotubes», *J. Clean. Prod.*, vol. 297, p. 126498, mag. 2021, doi: 10.1016/j.jclepro.2021.126498.
37. M. Srinivasan e T. White, «Degradation of Methylene Blue by Three-Dimensionally Ordered Macroporous Titania», *Environ. Sci. Technol.*, vol. 41, fasc. 12, pp. 4405–4409, giu. 2007, doi: 10.1021/es070160b.
38. M. H. Abdellah, S. A. Nosier, A. H. El-Shazly, e A. A. Mubarak, «Photocatalytic decolorization of methylene blue using TiO<sub>2</sub>/UV system enhanced by air sparging», *Alex. Eng. J.*, vol. 57, fasc. 4, pp. 3727–3735, dic. 2018, doi: 10.1016/j.aej.2018.07.018.
39. N. K. Sethy, Z. Arif, P. K. Mishra, e P. Kumar, «Green synthesis of TiO<sub>2</sub> nanoparticles from *Syzygium cumini* extract for photo-catalytic removal of lead (Pb) in explosive industrial wastewater», *Green Process. Synth.*, vol. 9, fasc. 1, pp. 171–181, feb. 2020, doi: 10.1515/gps-2020-0018.
40. V. De Matteis, M. Cascione, e R. Rinaldi, «Titanium dioxide: antimicrobial surfaces and toxicity assessment», in *Titanium Dioxide (TiO<sub>2</sub>) and Its Applications*, Elsevier, 2021, pp. 373–393. doi: 10.1016/B978-0-12-819960-2.00010-9.
41. K. S. Venkatesh *et al.*, «Facile one step synthesis of novel TiO<sub>2</sub> nanocoral by sol–gel method using Aloe vera plant extract», *Indian J. Phys.*, vol. 89, fasc. 5, pp. 445–452, mag. 2015, doi: 10.1007/s12648-014-0601-8.
42. F. Pellegrino, E. Ortel, J. Mielke, R. Schmidt, V. Maurino, e V.-D. Hodoroba, «Customizing New Titanium Dioxide Nanoparticles with Controlled Particle Size and Shape Distribution: A Feasibility Study Toward Reference Materials for Quality Assurance of Nonspherical Nanoparticle Characterization», *Adv. Eng. Mater.*, vol. 24, fasc. 6, p. 2101347, giu. 2022, doi: 10.1002/adem.202101347.
43. A. Almomen *et al.*, «In Vitro Safety Assessment of In-House Synthesized Titanium Dioxide Nanoparticles: Impact of Washing and Temperature Conditions», *Int. J. Mol. Sci.*, vol. 24, fasc. 12, p. 9966, giu. 2023, doi: 10.3390/ijms24129966.
44. S. Syamsol Bahri *et al.*, «Review on recent advance biosynthesis of TiO<sub>2</sub> nanoparticles from plant-mediated materials: characterization, mechanism and application», *IOP Conf. Ser. Mater. Sci. Eng.*, vol. 1142, fasc. 1, p. 012005, apr. 2021, doi: 10.1088/1757-899X/1142/1/012005.
45. C. Guillard, H. Lachheb, A. Houas, M. Ksibi, E. Elaloui, e J.-M. Herrmann, «Influence of chemical structure of dyes, of pH and of inorganic salts on their photocatalytic degradation by TiO<sub>2</sub> comparison of the efficiency of powder and supported TiO<sub>2</sub>», *J. Photochem. Photobiol. Chem.*, vol. 158, fasc. 1, pp. 27–36, mag. 2003, doi: 10.1016/S1010-6030(03)00016-9.
46. M. Zhang, L. Shi, S. Yuan, Y. Zhao, e J. Fang, «Synthesis and photocatalytic properties of highly stable and neutral TiO<sub>2</sub>/SiO<sub>2</sub> hydrosol», *J. Colloid Interface Sci.*, vol. 330, fasc. 1, pp. 113–118, feb. 2009, doi: 10.1016/j.jcis.2008.10.038.
47. V. De Matteis, M. Cascione, C. C. Toma, P. Pellegrino, L. Rizzello, e R. Rinaldi, «Tailoring Cell Morphomechanical Perturbations Through Metal Oxide Nanoparticles», *Nanoscale Res. Lett.*, vol. 14, fasc. 1, p. 109, dic. 2019, doi: 10.1186/s11671-019-2941-y.
48. A. K. John, S. Palaty, e S. S. Sharma, «Greener approach towards the synthesis of titanium dioxide nanostructures with exposed {001} facets for enhanced visible light photodegradation of organic pollutants», *J. Mater. Sci. Mater. Electron.*, vol. 31, fasc. 23, pp. 20868–20882, dic. 2020, doi: 10.1007/s10854-020-04602-1.

49. A. Di Paola, M. Bellardita, e L. Palmisano, «Brookite, the Least Known TiO<sub>2</sub> Photocatalyst», *Catalysts*, vol. 3, fasc. 1, pp. 36–73, gen. 2013, doi: 10.3390/catal3010036.
50. D. A. H. Hanaor e C. C. Sorrell, «Review of the anatase to rutile phase transformation», *J. Mater. Sci.*, vol. 46, fasc. 4, pp. 855–874, feb. 2011, doi: 10.1007/s10853-010-5113-0.
51. D. L. Liao, G. S. Wu, e B. Q. Liao, «Zeta potential of shape-controlled TiO<sub>2</sub> nanoparticles with surfactants», *Colloids Surf. Physicochem. Eng. Asp.*, vol. 348, fasc. 1–3, pp. 270–275, set. 2009, doi: 10.1016/j.colsurfa.2009.07.036.
52. Y. Wei, M. V. Tokina, A. V. Benderskii, Z. Zhou, R. Long, e O. V. Prezhdo, «Quantum dynamics origin of high photocatalytic activity of mixed-phase anatase/rutile TiO<sub>2</sub>», *J. Chem. Phys.*, vol. 153, fasc. 4, p. 044706, lug. 2020, doi: 10.1063/5.0014179.
53. S. Shen, X. Wang, T. Chen, Z. Feng, e C. Li, «Transfer of Photoinduced Electrons in Anatase–Rutile TiO<sub>2</sub> Determined by Time-Resolved Mid-Infrared Spectroscopy», *J. Phys. Chem. C*, vol. 118, fasc. 24, pp. 12661–12668, giu. 2014, doi: 10.1021/jp502912u.
54. J. Zhang, M. Vasei, Y. Sang, H. Liu, e J. P. Claverie, «TiO<sub>2</sub>@Carbon Photocatalysts: The Effect of Carbon Thickness on Catalysis», *ACS Appl. Mater. Interfaces*, vol. 8, fasc. 3, pp. 1903–1912, gen. 2016, doi: 10.1021/acsami.5b10025.

**Disclaimer/Publisher’s Note:** The statements, opinions and data contained in all publications are solely those of the individual author(s) and contributor(s) and not of MDPI and/or the editor(s). MDPI and/or the editor(s) disclaim responsibility for any injury to people or property resulting from any ideas, methods, instructions or products referred to in the content.